Excitation function and isomeric cross-section ratio for the ^{61}Ni$(p,\alpha)^{58}$Co^{m,g} process

S. Sudár,[1,2] F. Szelecsényi,[1] and S. M. Qaim[1]

[1]*Institut für Nuklearchemie, Forschungszentrum Jülich GmbH, 52425 Jülich, Federal Republic of Germany*

[2]*Institut of Experimental Physics, Kossuth University, H-4001 Debrecen, Hungary*

(Received 28 June 1993)

Excitation functions were measured by the stacked-foil technique for ^{61}Ni$(p,\alpha)^{58}$Co^{m} and ^{61}Ni$(p,\alpha)^{58}$Co^{m+g} reactions using 88.84% enriched ^{61}Ni from threshold up to 18.6 MeV. Thin samples of ^{61}Ni were prepared by electrodeposition on gold foils. The radioactivity of the activation products was determined via high resolution x- and γ-ray spectrometry. From the measured experimental data isomeric cross-section ratios $[\sigma_m/\sigma_{m+g}]$ were deduced. Statistical model calculations taking into account precompound effects were performed for the strong ^{61}Ni(p,xn) channels as well as for the weak ^{61}Ni(p,α) process. The experimental ^{61}Ni(p,xn) and ^{61}Ni(p,α) excitation functions are described well by the calculation over the whole investigated energy range. The isomeric cross-section ratio for the isomeric pair ^{58}Co^{m,g} formed in the ^{61}Ni(p,α) process is also reproduced well by the model calculation, provided the input level scheme and the spin distribution are properly taken into account.

PACS number(s): 25.40.Ep, 24.60.Dr

Studies of excitation functions of nuclear reactions are of considerable importance for testing nuclear models. Of special interest are investigations on isomeric cross-section ratios, particularly as a function of energy, since they should depict the effect of nuclear spin. Model calculations of the isomeric states have to account for more detail and, furthermore, depend critically on the input level scheme of the residual nucleus (cf. Refs. [1,2]). In this work we chose to investigate the ^{61}Ni$(p,\alpha)^{58}$Co^{m,g} process, where special techniques of sample preparation and radioactivity measurement were required. The aim was to test the predictive power of the model calculation.

Excitation functions were measured by the activation method using the stacked-foil technique, described in several publications from Jülich (cf. Refs. [3–5]). Some salient features relevant to the present measurements are described below.

An electroplating method was used to prepare thin ^{61}Ni samples on gold foils of thickness 4×10^{-2} g/cm^2 (cf. Ref. [5]). The percentage of isotopic composition of the enriched nickel was ^{58}Ni(3.45), ^{60}Ni(6.12), ^{61}Ni(88.84), ^{62}Ni(1.4), and ^{64}Ni(0.2). The thickness of the deposited layer ranged from 4×10^{-4} g/cm^2 to 1.2×10^{-3} g/cm^2 and had a diameter of 12 mm. Several Al and Cu foils were used as energy degraders and beam current monitors. All the samples and foils were individually weighed before irradiation.

All the irradiations were carried out with the external beam of the Compact Cyclotron CV28 of KFA Jülich using primary proton energies of 18.7 and 14.9 MeV. The area of the bombarding beam was decreased to about 1 mm^2, i.e., a well focused beam was used. The beam current was measured by a Faraday cup and was also monitored through monitor reactions induced in ^{nat}Cu foils. Some Al foils were inserted for energy degradation which was calculated according to Williamson, Boujot, and Pickard [6].

For studying the ^{61}Ni$(p,\alpha)^{58}$Co^{m} reaction, four stacks,

each containing 3–4 ^{61}Ni samples, some Al and Cu foils were irradiated for 1–5 h at beam currents of 150–200 nA. The thickness of the Al energy degraders was varied in each irradiation to get an energy overlap of 1–2 MeV between the different stacks. Two monitor reactions, viz. ^{63}Cu$(p,n)^{63}$Zn and ^{63}Cu$(p,2n)^{62}$Zn were used for measurement of proton energy and beam current (cf. Refs. [5,7]). For measurements on ^{58}Co^{m+g} 13 samples of ^{61}Ni were activated in the form of a stack together with Al degraders and Cu monitor foils for 5 h at a proton beam current of 200 nA. The beam was monitored as described above.

The radioactivity of the ^{61}Ni$(p,\alpha)^{58}$Co^{m+g} reaction product ($T_{1/2} = 70.92d$, $E_\gamma = 810.8$ keV, $I_\gamma = 99.5\%$) as well as of the monitor reaction products was determined via standard HPGe detector γ-ray spectrometry. In the case of ^{58}Co all the measurements were started after complete decay of the ^{58}Co^{m} ($T_{1/2} = 9.15$ h) to the ground state. The detector was coupled to an Ortec MCA Plug-In card which was connected to IBM-compatible PC-AT. The energy and efficiency calibration of the system was done using standard (error $<3\%$) calibration sources ^{60}Co (Amersham), ^{133}Ba(PTB), ^{134}Cs(PTB), and ^{152}Eu(PTB). The detector-source distances were 10, 40, and 50 cm. The dead times were kept below 3%; however, in the case of some monitor foils it was 5%. The peak area analysis was done using a detailed peak analyzing program developed for IBM-PC.

The radioactivity of the ^{61}Ni$(p,\alpha)^{58}$Co^{m} reaction product was somewhat difficult to measure. This metastable state decays with a half-life of 9.15 h to the ground state via isomeric transition (IT) which is highly converted. We therefore performed Si(Li)-detector x-ray spectrometry utilizing the x rays of cobalt (K_α, 6.9 keV; K_β, 7.6 keV). The calibration of this system was done using standard sources ^{57}Co(PTB), ^{241}Am (Amersham), and ^{55}Fe(Amersham). The source-detector distance was 2 cm. From the count rates of the product activities the de-

cay rates were obtained using decay data (cf. Ref. [8]) and the efficiency of the detector. The cross sections were then calculated using the well-known activation formula.

The total errors in the cross sections were obtained by summing up quadratically the possible individual relative errors: counting statistics 1–5 %; detector efficiency 5% (for $^{58}Co^{m+g}$) and 8% (for $^{58}Co^m$); decay data <3%; number of target nuclei 8%, and incident bombarding particle intensity 8%. The total estimated errors in the cross sections were ~15% for $^{58}Co^m$ and ~13% for $^{58}Co^{m+g}$. The energy scale error was estimated to be ±0.2 MeV at 18.6 MeV, ±0.5 MeV at 10 MeV, and ±0.6 MeV at 6.0 MeV.

Cross-section calculations were done using the statistical model taking into account the preequilibrium effects. The calculational code STAPRE [9] was used. Direct interactions were not considered but their contribution should be <10%. Neutron, proton, alpha, and deuteron emission was taken into account and the transmission coefficients for these particles were calculated by the optical model code SCAT-2 [10]. The parameters for the optical mode (OM) were chosen from a global parameter set. For the neutron the OM parameter set of Becchetti and Greenlees [11] while for proton and deuteron those of Perey [12] were used. In the case of alpha particles a modified set of the OM parameters of McFadden and Satchler [13] (modified by Uhl et al. [14]) was used. For the energy and mass dependence of the effective matrix element, $|M|^2 = F_M A^{-3} E^{-1}$ formula was used with the value of $F_M = 500$. The separation energies of the emitted particles were taken from Ref. [15].

The energies, spins, parities, and branching ratios of the discrete levels were selected from the Nuclear Data Sheets [16]. In the continuum region the level density was calculated by the back-shifted formula [17] with the level density parameter given in Ref. [17]. In cases where these parameters were not available they were estimated from the systematics and from the values of the neighboring isotopes. Occasionally, the level density parameters a and Δ were varied within their uncertainties to check their effect on the cross sections. The spin distribution of the level density was characterized by the ratio of the effective moment of inertia Θ_{eff} to rigid body moment of inertia Θ_{rig} ($\eta = \Theta_{eff}/\Theta_{rig}$). The calculations were performed for $\eta = 1.0$ and 0.5 to investigate its effect on the isomeric cross-section ratio. The transmission coefficients of photons were calculated from the gamma-ray strength functions. For the $E1$ radiation the Brink-Axel model with global parameters ($\Gamma\gamma = 0.573$ eV), while for the $M1$, $E2$, $M2$, $E3$, and $M3$ radiation the Weisskopf model was used.

The measured cross sections with the estimated total errors are given in Table I. A far as we know, these measurements describe a first systematic study of the (p,α) process on ^{61}Ni using highly enriched target isotope. The data for $^{61}Ni(p,\alpha)^{58}Co^m$ reaction are reported for the first time. An earlier measurement (cf. Ref. [18]) on the $^{61}Ni(p,\alpha)^{58}Co^{m+g}$ process was done using natural Ni and the data were given only in a graphical form. Although those data are somewhat higher than our values, taking account the error limit of 15–20 % the agreement is

TABLE I. Cross sections for the $^{61}Ni(p,\alpha)^{58}Co^{m+g}$ and $^{61}Ni(p,\alpha)^{58}Co^m$ reactions.

E (MeV)	σ_{m+g} (mb)	σ_m (mb)
5.3±0.6	0.09±0.3	
6.3±0.6	0.96±0.13	0.37±0.05
6.5±0.6		1.15±0.23
7.3±0.5	5.21±0.66	2.00±0.31
8.0±0.5		6.14±0.86
8.4±0.5	16.9±2.1	6.50±0.93
8.9±0.5		8.9±1.3
9.5±0.5	26.8±3.4	14.2±2.0
10.3±0.4		18.7±2.7
10.7±0.4	41.3±5.2	
11.8±0.4	50.6±6.3	
12.0±0.4		24.9±3.5
12.8±0.4	52.2±6.5	
13.3±0.4		32.4±4.6
13.8±0.3	52.8±6.6	
14.0±0.3		31.8±4.4
14.8±0.3	57.1±7.2	
15.2±0.3		35.1±5.0
16.1±0.3	58.2±7.3	
16.9±0.3		31.9±4.5
17.4±0.2	44.1±5.5	
18.5±0.2	40.2±5.0	27.7±3.9

good.

In nuclear model calculations we aimed at a simultaneous reproduction of the available experimental data which comprise strong reaction channels, namely, $^{61}Ni(p,n)^{61}Cu$ and $^{61}Ni(p,2n)^{60}Cu$ reactions (cf. Ref. [19]), and the much weaker $^{61}Ni(p,\alpha)^{58}Co^{m,g}$ process (this work).

The results on the $^{61}Ni(p,xn)^{60,61}Cu$ reactions are shown in Fig. 1. For both reactions the measured and calculated data are in good agreement, depicting that the neutron emission is described well by the statistical model. A small deviation between the measured and calculated data below 6 MeV may indicate inaccuracy in the global OM parameters.

The results for the $^{61}Ni(p,\alpha)^{58}Co^m$ and

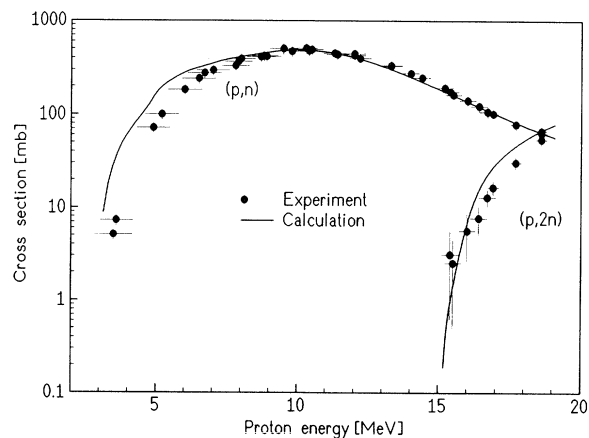FIG. 1. Measured and calculated excitation functions of the $^{61}Ni(p,n)^{61}Cu$ and $^{61}Ni(p,2n)^{60}Cu$ reactions (experimental data from Ref. [19], model calculation (this work)).
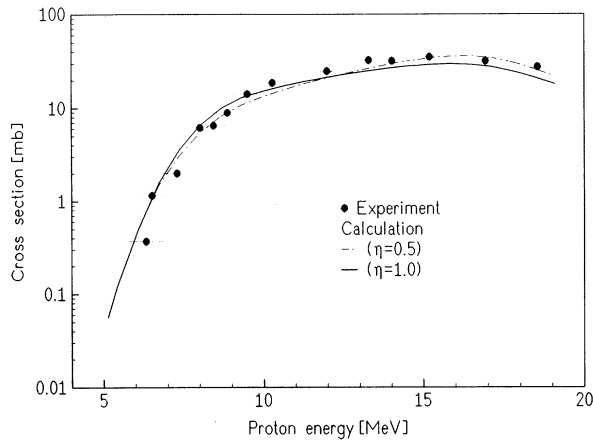
FIG. 2. Measured and calculated cross sections for the $^{61}\mathrm{Ni}(p,\alpha)^{58}\mathrm{Co}^m$ reaction.

FIG. 4. Comparison of the experimental data for the $^{61}\mathrm{Ni}(p,\alpha)^{58}\mathrm{Co}^{m+g}$ process with the results of nuclear model calculations using different model parameters.

$^{61}\mathrm{Ni}(p,\alpha)^{58}\mathrm{Co}^{m+g}$ processes are shown in Figs. 2 and 3, respectively. Calculations were performed for two cases ($\eta=1$ and 0.5); the difference was, however, very small. A comparison of the experimental and theoretical results shows good agreement over the investigated energy range.

To check the effect of input parameters, the model calculation was performed using slightly modified values (by 10%) of the level density in the neutron channel and optical model parameters of the alpha channel. Three examples of those calculations for the total $^{61}\mathrm{Ni}(p,\alpha)^{58}\mathrm{Co}^{m+g}$ activation cross section are given in Fig. 4. In one case the nuclear radius parameter for the $^{58}\mathrm{Ni}$ $r_R=r_V=r_C=1.445$ fm was used (continuous line), and in the other $r_R=r_V=r_C=1.300$ fm (dashed line). It can be seen that the cross section varies by a factor of 2 near the threshold and 10–20 % at the maximum. The third case consisted of change in the level density parameter of the neutron channel (for $^{61}\mathrm{Cu}$). The results are also shown in Fig. 4 [$a=6.50$ (continuous line) and $a=5.99$ (dotted line)]. The effect is significant only above 10 MeV and causes a change of 20–30 % in the (p,α) cross section.
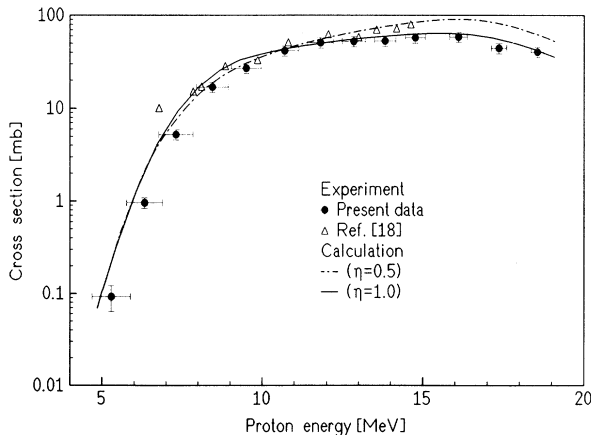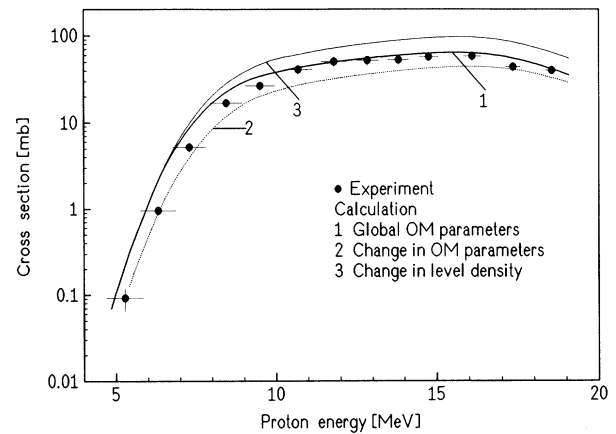
The measured and calculated isomeric cross section ratios (σ_m/σ_{m+g}) for the isomeric pair $^{58}\mathrm{Co}^{m,g}$ formed in the $^{61}\mathrm{Ni}(p,\alpha)$ process are shown in Fig. 5 as a function of proton energy. The ratio is low at low incident proton energies but increases with the increasing energy. This trend is in agreement with the known behavior where the yield of the high spin isomer increases with the increasing incident particle energy. The calculated ratio was found to be practically independent of the level density, optical model parameters, and gamma-ray strength functions. It was mainly determined by the input level scheme and spin distribution through the effective moment of inertia. The effect of the multipolarity of the gamma transition was tested by changing the maximum of multipolarity from 3 to 1 and 2, which caused only 0–5 % variation in the isomeric cross-section ratio. Therefore, the deviation between the calculated and the measured ratios at high energies cannot be explained by different relative contributions of the different gamma transitions (dipole, quad-
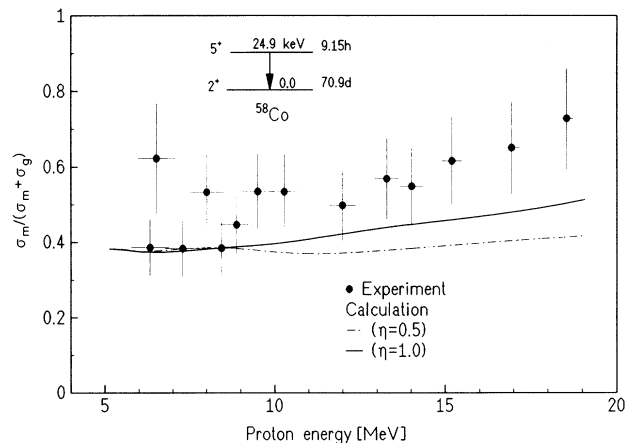

FIG. 3. Measured and calculated cross sections for the $^{61}\mathrm{Ni}(p,\alpha)^{58}\mathrm{Co}^{m+g}$ process.

FIG. 5. Measured and calculated isomeric cross-section ratios (σ_m/σ_{m+g}) for the $^{61}\mathrm{Ni}(p,\alpha)^{58}\mathrm{Co}^{m,g}$ process as a function of proton energy. The spins and parities of the two isomeric levels concerned are shown.

rupole, etc.) The results are shown for two values of η and it can be seen that $\eta = 1.0$ gives better agreement with the experimental data. Similar results were presented in Refs. [20,21] for neutron induced reactions, indicating that in this mass region the effective moment of inertia is equal to the rigid body value.

[1] S. M. Qaim, A. Mushtaq, and M. Uhl, Phys. Rev. C 38, 645 (1988).

[2] N. I. Molla, S. M. Qaim, and M. Uhl, Phys. Rev. C 42, 1540 (1990).

[3] R. Weinreich, O. Schult, and G. Stöcklin, Int. J. Appl. Radiat. Isotopes 25, 535 (1977).

[4] S. M. Qaim, G. Stöcklin, and R. Weinreich, Int. J. Appl. Radiat. Isotopes 28, 947 (1974).

[5] H. Piel, S. M. Qaim, and G. Stöcklin, Radiochim. Acta 57, 1 (1992).

[6] C. F. Williamson, J. P. Boujot, and J. Pickard, Report No. CEA-R-3042, 1966 (unpublished).

[7] O. Schwerer and K. Okamoto, IAEA Report No. INDC(NDS)-218/GZ, Vienna, Austria, 1989 (unpublished).

[8] E. Browne and R. B. Firestone, in *Table of Radioactive Isotopes*, edited by V. S. Shirley (Wiley, London, 1986).

[9] M. Uhl and B. Strohmaier, "Computer Code for Particle Induced Activation Cross Section and Related Quantities," IRK Report No. 76/01, 1976 (unpublished).

[10] O. Bersillon, Report No. CEA-N-2227, 1981 (unpublished).

[11] F. D. Becchetti and G. W. Greenlees, Phys. Rev. 182, 1190 (1969).

[12] F. G. Perey, Phys. Rev. 131, 745 (1962).

[13] L. McFadden and G. R. Satchler, Nucl. Phys. 84, 177 (1966).

[14] M. Uhl, H. Gruppelaar, H. A. J. van der Kamp, J. Kopecky, and D. Nierop, in *Proceedings of the International Conference on Nuclear Data for Science and Technology*, Jülich, 1991, edited by S. M. Qaim (Springer Verlag, Berlin, 1992), p. 924.

[15] A. H. Wapstra and K. Bos, Atm. Data Nucl. Data Tables 19, 215 (1977).

[16] T. W. Burrows and M. R. Bhat, Nucl. Data Sheets 47, 1 (1986); L. K. Peker, *ibid.* 42, 457 (1984); L. P. Ekström and J. Lyttkens, *ibid.* 38, 463 (1983); R. L. Auble, *ibid.* 28, 103 (1979).

[17] W. Dilg, W. Schantl, H. Vonach, and M. Uhl, Nucl. Phys. A217, 269 (1973).

[18] S. Tanaka, M. Furukawa, and M. Chiba, J. Inorg. Nucl. Chem. 34, 2429 (1972).

[19] F. Szelecsényi, G. Blessing, and S. M. Qaim, Appl. Radiat. Isotopes 44, 575 (1993).

[20] R. Fischer, G. Traxler, M. Uhl, and H. Vonach, Phys. Rev. C 30, 72 (1984).

[21] R. Fischer, G. Traxler, M. Uhl, H. Vonach, and P. Maier-Komor, Phys. Rev. C 34, 460 (1986).